

Study of the photon identification efficiency with ALICE photon spectrometer^{*}

MAO Ya-Xian(毛亚显)¹⁾ ZHOU Dai-Cui(周代翠)²⁾

XU Chun-Cheng(徐春成) YIN Zhong-Bao(殷中宝)

(Institute of Particle Physics, Central China Normal University, Wuhan 430079, China)

Abstract The efficiency for the detection and identification of photons with the ALICE PHOTON Spectrometer PHOS has been studied with the Monte-Carlo generated data. In particular, the influence on the efficiency of the PHOS-module edge-effect and of the material in front of PHOS have been examined.

Key words ALICE experimental simulation, photon detection, identification efficiency, detector edge effect and photon conversion

PACS 24.10.Lx, 25.20.Lj, 29.85.+e, 29.40.Vj

1 Introduction

Much efforts have been involved in recent years, both theoretically and experimentally, to investigate a new state of matter, the quark-gluon plasma (QGP)^[1], which might be formed in high-energy nucleus-nucleus (A - A) collisions. This state of matter is thought to exist in the early universe shortly after the Big-Bang. Several signals have been advocated to reveal the formation of the QGP and inspect its properties, such as strangeness enhancement, J/ψ suppression, direct photon enhancement, heavy quark energy loss and so on.

The production of direct photons is one of the most promising probes to test the dynamical properties of the colliding system^[2, 3]. Unlike hadrons, photons only interact electromagnetically and consequently have a long mean free path, which is typically much larger than the transverse size of the matter created in nuclear collisions. Therefore, photons will escape from the system with undisturbed information about the physical conditions under which they were created^[4].

Photons are produced during the entire duration of the collision. In the initial phase, prompt photons are produced in hard scattering of initial-state

partons, mainly through gluon Compton scattering ($qg \rightarrow q\gamma$) and quarks annihilation ($q\bar{q} \rightarrow g\gamma$), and, at the next-to-leading-order in the fragmentation of final-state partons ($E_\gamma \lesssim 20$ GeV). The QGP is at the origin of direct photons ($2 \lesssim E_\gamma \lesssim 10$ GeV) through thermal radiation arising from in-medium Compton and annihilation processes between thermalized partons, through conversion of hard scattered partons traversing the medium^[5], and through bremsstrahlung of hard scattered quarks traversing the medium^[6]. Direct photons are finally also produced by thermal radiation of the hadron gas in the late stage of the collision until freeze-out time. The dominant source of photons is however due to decay photons (mainly from neutral pions) which constitute the main background of the direct photon measurement. The direct photon production in heavy-ion collisions has been investigated experimentally at SPS^[7] and RHIC^[8]. The most up-to-date theoretical predictions for the direct-photon production at RHIC and LHC energies can be found in Ref. [9] and references therein.

Proton-proton (p-p) collisions at $\sqrt{s} = 14$ TeV (and possibly at 900 GeV for a short run) and lead-lead (Pb-Pb) collisions at $\sqrt{s_{NN}} = 5.5$ TeV will become available at LHC in 2008/09. The Large Ion

Received 3 September 2007

^{*} Supported by Ministry of Science & Technology of China (2008CB317106), National Natural Science Foundation of China (10575044, 10635020), Key Project of Chinese Ministry of Education (306022, IRT0624)

1) E-mail: maoyx@iopp.cnu.edu.cn

2) E-mail: dczhou@mail.cnu.edu.cn

Collider Experiment (ALICE) at LHC is dedicated to the study of the properties of the QGP and the structure of the QCD phase diagram^[10, 11]. The PHOTon Spectrometer (PHOS)^[12] located in the central rapidity region of ALICE will detect photons and allow to discriminate direct and decay photons over a wide dynamic range, $0.5 \lesssim E_\gamma \lesssim 100$ GeV.

Our present work focuses on the study of prompt-photon detection and identification efficiency in p-p collisions, making use of the rather clean environment for photon detection. The study will be extended to the study of prompt photon produced in nucleus-nucleus collisions at $\sqrt{s_{NN}}=5.5$ TeV.

Prompt photons are generated by the Pythia event generator^[13, 14] and the response of the detector by the GEANT3 transport model^[15]. Both software packages are integrated in the ALICE framework AliRoot^[16], for simulation, reconstruction and analysis. In the analysis of the Monte-Carlo data, photons detected by PHOS are identified combining the information provided by the detector (shower shape, time of flight, charge particle veto). Factors affecting the photon detection and identification, such as detector-edge effects and photon conversion ($\gamma \rightarrow e^+e^-$) in the material in front of PHOS have been studied.

2 Photon spectrometer in ALICE

The ALICE detector will start to operate with p-p collisions at $\sqrt{s} = 900$ GeV and 14 TeV, and will pursue a genuine physics program making use of its unique capabilities for particle identification and tracking of charged particles down to very low momenta. Furthermore, measurements in p-p collisions will provide the base-line data for Pb-Pb. In ALICE, photons will be detected by PHOS. It is a single-arm electromagnetic spectrometer with high energy and position-resolution thanks to its high-granularity. It includes a highly segmented Electro Magnetic Calorimeter (EMCA) and a Charged-Particle Veto (CPV) detector, subdivided into five independent EMCA+CPV units, named PHOS modules. The modules are positioned on the bottom of the ALICE setup at a distance of 460 cm from the beam interaction point. They cover the pseudo-rapidity region $-0.12 \leq \eta \leq +0.12$ and span an azimuthal angle of 100 degrees, $220 \leq \phi \leq 320$ with respect to the beams axis. Each EMCA module consists of a matrix of 56×64 individual lead-tungstate (PbWO_4) scintillators ($2.2 \text{ cm} \times 2.2 \text{ cm} \times 18.0 \text{ cm}$). The light output of each scintillator is read out by a large area ($5 \text{ mm} \times 5 \text{ mm}$) avalanche photo diode coupled to a low noise charge sensitive preamplifier and shaper. The signal is then processed in a front-end

electronics card attached at the back of the detector. The readout circuits collect the information from a module and send the detector signals (amplitude and time with respect to a fixed reference measured for each crystal) and trigger information to the ALICE data acquisition system. Each module is associated with a charged particle detector positioned in front of the module and operated as a Charged Particle Veto (CPV) detector. The granularity of CPV matches the granularity of EMCA allowing the identification of the charge of particles hitting PHOS.

Material from other ALICE detectors positioned in front of PHOS causes secondary interactions of incident particles before they reach PHOS, thus, altering the detection and identification capabilities. The main mechanism to consider is photon conversion ($\gamma \rightarrow e^+e^-$). The edge effect, for photons impinging on the edge of a module, results in a loss of the shower, leaking outside the module. To suppose this effect, the fiducial acceptance of a module must be reduced by 7% ($2 \times (56 + 64) / 56 \times 64$).

3 Photon production and simulation configuration

We have focused the present study on the high-energy part of the photon spectrum, where the prompt photons provide the dominant contribution, thus, discarding the low energy photons directly originating from the QGP. Our ultimate purpose is to study the correlations between the prompt photons and the hadrons created in hard partonic scattering and to identify relevant observables sensitive to the properties of medium, such as jet quenching^[17]. Monte-Carlo events were generated with two configurations. In the first one, events with a single photon with energy distributed between 2 and 50 GeV were generated using the AliGenBox generator in AliRoot. The p-p events were generated by the Pythia generator (AliGenPythia in AliRoot) triggering on $2 \rightarrow 2$ processes with a prompt photon in the final state and involving a center-of-mass momentum transfer larger than 2 GeV/c for p-p events at 900 GeV/c and 10 GeV/c for p-p collisions at 14 TeV/c. In addition, only the events for which the direct photon points in the direction of PHOS have been retained. To study separately the edge effects we have considered two different geometries of PHOS. In the first one the generated photons illuminated the geometrical acceptance of all five modules and in the second one only the fiducial acceptance (excluding the edges, i.e. reducing the azimuth coverage from 20 deg to 16 deg and eta from 0.12 to 0.11) of a single module was illuminated.

The generated particles were tracked through the detector using the GEANT3 transport package. The reconstruction algorithm assembles all continuous hits, above a set deposited-energy threshold, in the scintillators belonging to the same PHOS module. The resulting cluster is assigned to the detection of a particle whose energy is the total deposited energy in the cluster and the position is the energy-weighted average of the individual scintillators position belonging to the cluster. The parameters of the reconstruction algorithms have been tuned to reproduce the performance (energy and position resolution) of a PHOS module measured with a test beam^[18]. The particle identification (PID) is achieved combining the two-dimensional shape of the clusters, the information delivered by the CPV and the time of flight information. Weights calculated following the statistical Bayesian approach^[19] and representing the probability that a given cluster is a particle of a given type (among photon, electron, charged hadron, neutral baryon), are attributed to the clusters.

4 Simulation results

The effects due to the edges have been estimated by comparing the simulation of single photon events where the photon illuminates the fiducial acceptance of one PHOS module (Excluding the edges) and the same simulation but with the photon illuminating the geometrical acceptance of PHOS. The efficiency has been calculated by dividing the number of reconstructed identified photons with the number of the generated photon (a flat distribution between 2 GeV and 50 GeV). Reconstructed clusters have been identified as photons by selecting the clusters with a photon PID weight larger than 0.9. All the detectors in

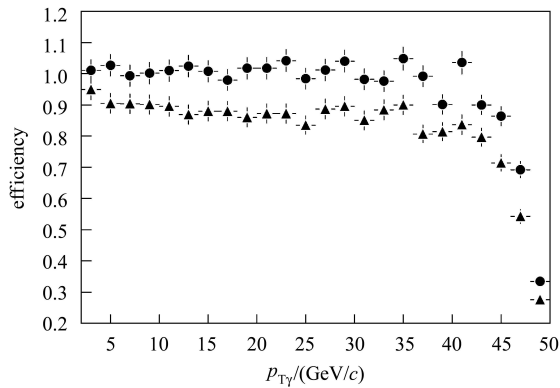


Fig. 1. PHOS photon detection and identification efficiency vs reconstructed transverse momentum p_T calculated from single photon events illuminating the fiducial acceptance on one PHOS module (full circles) and illuminating the geometrical acceptance of PHOS (up triangles).

front of PHOS in the ALICE set up (ITS, TPC, TRD and TOF) have been switched off in the simulation. The result (Fig. 1), shows that the PHOS detection efficiency of identified photons is equal to 1 over the entire energy range studied. The drop near the cut-off energy of the simulated photons is due to the detector response and the incomplete collection of the shower in EMCA (no re-calibration has been applied to the reconstructed cluster energy). When the acceptance is extended to the geometrical acceptance of the modules, the efficiency drops down to 0.9 (Fig. 1), i.e. a 10% reduction due to the edge effect.

When material is added in front of the PHOS modules, the efficiency (Fig. 2) drops moderately down to 0.8 when only ITS and TPC are considered (12% of radiation length) but drops drastically down to 0.6 when TRD and TOF are also taken into account (80% of radiation length average over the module acceptance). This drop scales with the amount of radiation length and the probability to convert a photon. Once converted, the identification algorithms reject the resulting cluster because of the CPV which recognizes the electrons.

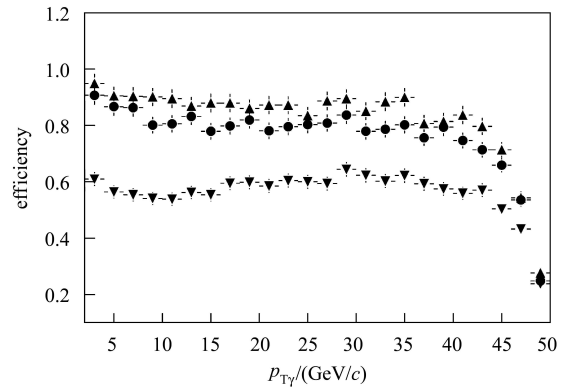


Fig. 2. PHOS photon detection and identification efficiency vs reconstructed transverse momentum p_T calculated from single photon events illuminating the geometrical acceptance of PHOS with no material in front (up triangles), with ITS and TPC in front (full circles) and with in addition TRD and TOF (down triangles).

The same results are obtained with the Pythia generated p-p events. The shape of the reconstructed photon spectrum is identical to the shape of the generated spectrum at 900 GeV/c (Fig. 3) as well as at 14 TeV/c (Fig. 4). The efficiency loss due to the material in front PHOS (Fig. 5) is well reproduced as well as the overall efficiency (Fig. 6) including edge and material effects and which is reduced to 0.5. Both effects can be seen by photons azimuthal distribution (Fig. 7) and the efficiency as a function of the polar angle (Fig. 8). These results have been obtained by

covering 4 modules and leaving the central module uncovered. The reduction due to the material can be obviously quantified. The edge effects can be identified by the low values of the efficiency at the edge of the modules.

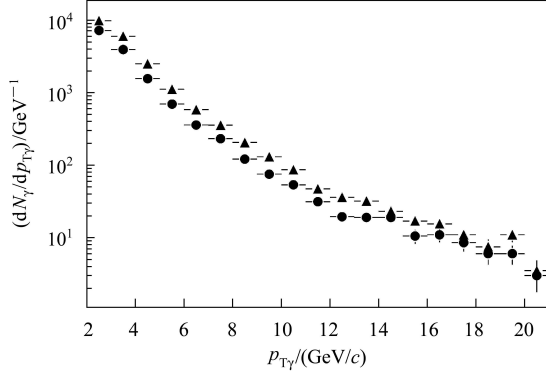


Fig. 3. Generated (up triangles) and reconstructed identified (full circles) photon spectrum obtained from Pythia p-p events at $\sqrt{s_{NN}} = 900$ GeV. The fiducial acceptance of one PHOS module was illuminated.

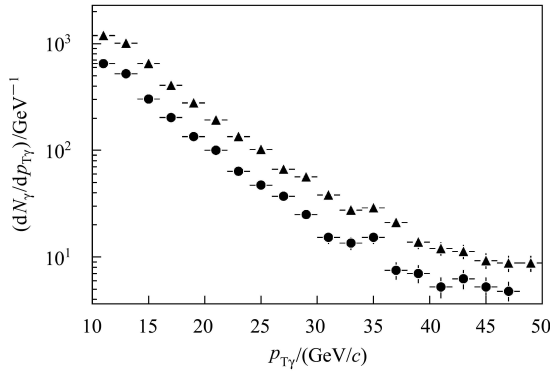


Fig. 4. Generated (up triangles) and reconstructed identified (full circles) photon spectrum obtained from Pythia p-p events at $\sqrt{s_{NN}} = 14$ TeV. The geometrical acceptance of PHOS was illuminated.

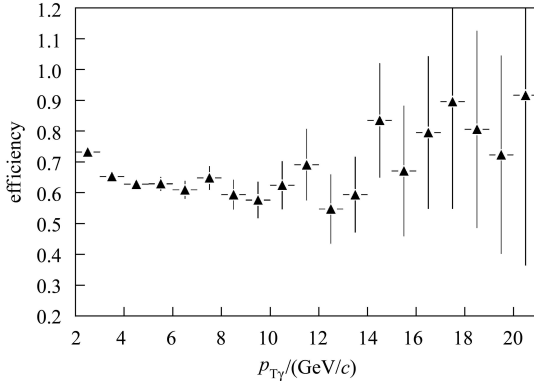


Fig. 5. PHOS photon detection and identification efficiency vs reconstructed transvers momentum p_T calculated from Pythia p-p events at $\sqrt{s_{NN}} = 900$ GeV. The fiducial acceptance of one PHOS module was illuminated.

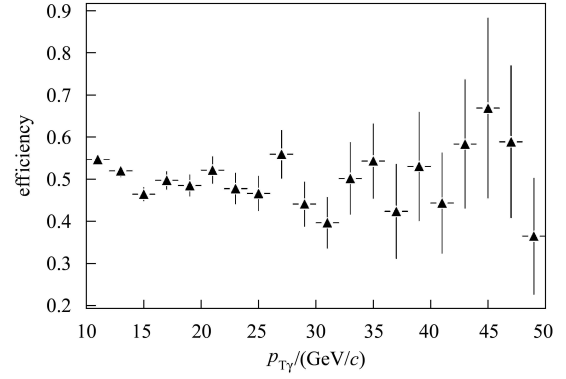


Fig. 6. PHOS photon detection and identification efficiency vs reconstructed transvers momentum p_T calculated from Pythia p-p events at $\sqrt{s_{NN}} = 14$ TeV. The geometrical acceptance of PHOS was illuminated.

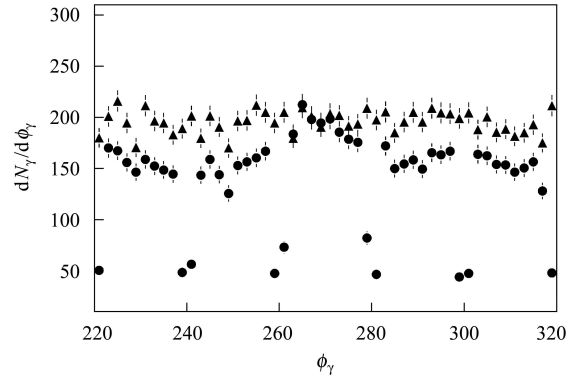


Fig. 7. Generated (up triangles) and reconstructed and identified (full circles) photon distribution vs azimuth angle from Pythia p-p events at $\sqrt{s_{NN}} = 14$ TeV. The geometrical acceptance of PHOS was illuminated.

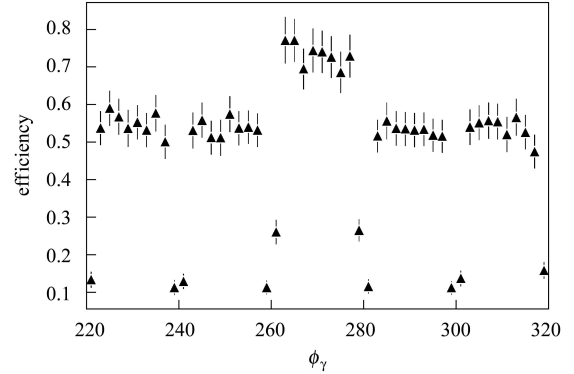


Fig. 8. PHOS photon detection and identification efficiency vs azimuth angle calculated from Pythia p-p events at $\sqrt{s_{NN}} = 14$ TeV. The geometrical acceptance of PHOS was illuminated.

5 Summary and discussion

We have studied with the Monte-Carlo data the performance of the PHOS photon spectrometer in the

ALICE experiment. From the simulations of events containing a single photon, we have calculated the efficiency of photon detection and identification given by the PHOS reconstruction and identification algorithm implemented in the ALICE AliRoot framework. We have shown that the intrinsic efficiency of a PHOS module is reduced by about 10% (to be compared to the ratio of edge crystals and crystals in one module equal to 7%) because of the leakage of the electromagnetic shower for photons impinging on the edge of the PHOS modules. The efficiency is

much more drastically reduced if material is covering the PHOS acceptance. Having TRD and TOF in front of PHOS will reduce the photon detection and identification efficiency down to 0.5 because of the photon conversion.

The authors gratefully acknowledge Professor Yves Schutz, Dr. Gustavo Conesa Balbastre, Dr. Yuri Kharlov and the ALICE/offline colleagues for their enthusiastic discussions and helps during the work.

References

- 1 Shuryak E V. Phys. Rep., 1980, **61**: 71
- 2 Shuryak E V. Sov. J. Nucl. Phys., 1978, **28**: 408
- 3 Peitzmann T, Thoma M H. Phys. Rep., 2002, **364**: 175
- 4 Kapusta J, Lichard P, Seibert D. Phys. Rev. D, 1991, **44**: 2774
- 5 Fries R J, Muller B, Srivastava D K. Phys. Rev. Lett., 2003, **90**: 132301
- 6 Turbide S, Gale C, Jeon S, Moore G D. Phys. Rev. C, 2005, **72**: 014906. [arXiv:hep-ph/0502248]
- 7 Heinz U W, Jacob M. arXiv:nucl-th/0002042
- 8 Adams J et al. (STAR Collaboration). Nucl. Phys. A, 2005, **757**(issues 1-2): 102—183
- 9 Sinha B. 'Last Call for Predictions' workshop, CERN, May 15, <http://fpaxp1.usc.es/nesor/defseminars.html>
- 10 ALICE Collaboration, ALICE-PPR. J. Phys. G; Nucl. Part. Phys., 2004, **30**: 1517—1763
- 11 ALICE Collaboration, ALICE-PPR. J. Phys. G; Nucl. Part. Phys., 2006, **32**: 1295—2040
- 12 ALICE Collaboration, ALICE-TDR. CERN/LHCC, 1999, **99-4**: 1—173
- 13 Sjostrand T, Loonblad L, Mrenna S. hep-ph/0108264, 2001
- 14 Sjostrand T et al. Comput. Phys. Commun., 2001, **135**: 238—259
- 15 GEANT3. <http://wwwasd.web.cern.ch/wwwsd/geant>
- 16 AliRoot: ALICE offline project. <http://aliceinfo.cern.ch/Offline>
- 17 WANG X N. Phys. Lett. B, 2004, **579**: 299 (nucl-th/0307036)
- 18 Test Beam. <http://aliceinfo.cern.ch/Collaboration>
- 19 Conesa G et al. Internal Note/ALICE-INT-2005-016 version 1.0, 2005